Polarizabilities of individual molecules and ions in liquids from first principles

2008 J. Phys.: Condens. Matter 20 494207

(http://iopscience.iop.org/0953-8984/20/49/494207)

J. Phys.: Condens. Matter **20** (2008) 494207 (8pp) doi:10.1088/0953-8984/20/49/494207

Polarizabilities of individual molecules and ions in liquids from first principles

M Salanne[1,2], R Vuilleumier[2,3,4], P A Madden[5], C Simon[1,2], P Turq[1,2] and B Guillot[2,4]

[1] UPMC Université Paris 06, UMR 7612, LI2C, F-75005, Paris, France
[2] CNRS, F-75005, Paris, France
[3] Département de Chimie, Ecole Normale Supérieure, F-75005, Paris, France
[4] UPMC Université Paris 06, UMR 7600, LPTMC, F-75005, Paris, France
[5] School of Chemistry, University of Edinburgh, Edinburgh EH9 3JJ, UK

E-mail: mathieu.salanne@upmc.fr

Received 29 July 2008
Published 12 November 2008
Online at stacks.iop.org/JPhysCM/20/494207

Abstract

Dipole polarizabilities of individual ionic or molecular species are computed in three different liquid systems: liquid water, molten salts and magmatic melts, the last two belonging to the class of ionic liquids. The method is based on a purely first-principles procedure. The liquid water polarizability tensor is found to be nearly isotropic in the molecular framework. Important environmental effects occur in the two ionic systems when the nature and concentration of the cations are changed. The results of these calculations will be useful in the building of interaction potentials which include polarization effects.

(Some figures in this article are in colour only in the electronic version)

1. Introduction

The electronic polarizability of a molecule or an ion is a measure of the relative tendency of its electron cloud to be distorted from its normal shape by an electric field. On the macroscopic scale it affects the optical properties of a material by determining its refractive index, and fluctuations in the polarizability contribute to the light-scattering spectrum. On the molecular scale, in a non-metallic condensed phase, any species sits in an electric field due to its neighbors and the resulting polarization is an important contribution to the total interaction energy.

Apart from optical properties, it is however difficult to estimate the influence of polarization effects on the physical properties of a liquid. Recently, computer simulations have emphasized their importance in two very different applications. Firstly, several groups have shown that the behavior of ions at the air/water interface are strongly affected when a polarization term is added to the interaction potential [1–3]. It affects the affinity for the interface for soft monovalent anions. The results on the surface composition of alkali halide aqueous solutions have recently been confirmed experimentally by grazing incidence x-ray diffraction [4]. More generally, substantial effort has been devoted to the study of specific ion effects since the pioneering work of Hofmeister in the late 19th century [5]. The main objective is to rationalize the effects of the nature of a salt on the solubility of proteins. Again, it has been shown that the polarizability of anions and cations plays an important role. Ionic liquids constitute another class of materials in which polarizability has to be taken into account for an accurate description of structural and dynamical properties. Such potentials have been developed and tested for molten chlorides [6, 7], fluorides [8, 9] and oxides [10]. A schematic view of the polarization effects on the structure of a melt is provided on figure 1. In this example, two SiO_4 units are connected together through a bridging O^{2-} anion. When polarization effects are not accounted for in the model, the anion tends to lie along the cation–cation axis (its position corresponds to the white circle in the figure) and screens the repulsion between the highly charged cation. When the anion is polarizable a dipole is induced if it lies off-axis, thus inducing a supplementary screening. The Si–O–Si angle can therefore be reduced (the anion position now is the black circle), consistently with the experimental results [11]. In all ionic melts, important relationships between structure and dynamics can be established [12, 13]; the polarizable models are able to reproduce the structure and dynamical properties of systems with polyvalent cations, which the simple pair potentials cannot.

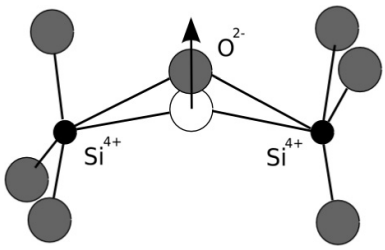

Figure 1. A schematic view of the polarization effect on the structure of an ionic melt. In this example, two isolated SiO_4 units are connected together through a bridging O^{2-} anion. The white circle is the anion position in a non-polarizable model, and the black one in a polarizable model. The arrow corresponds to the induced dipole on the anion in the polarizable model.

In order to improve the prediction of material properties, a major effort has been made to develop polarizable interaction potentials in the last few years. Compared to the almost parameter free first-principles molecular dynamics [14, 15], in which electrons are explicitly represented, large simulation cells and long simulation times can be reached, and quantities like the viscosity or the electric conductivity can be evaluated. A drawback though, is that additional parameters are introduced in the interaction potential, and it is not always straightforward to choose them in a physically meaning way. In the case of the polarizability, gas phase values have often been measured experimentally, but liquid phase ones remain undetermined. It is therefore of primary interest to develop a theoretical method to compute accurately the polarizability of any species in a liquid. So far, there has been relatively little work on ions in molecular media or on solvent effects on the molecular polarizability. Jungwirth and Tobias have examined solvent effects on ion polarizability in aqueous solvents [16–18]. Their approach consists of studying the response of the electron cloud to a potential arising from a system of point charges representing the electrostatic contribution from the solvent. They therefore bypass the calculation of multipole-induced-multipole contributions to the cluster polarizability. Morita has proposed another scheme for dealing with molecular systems [19]. His calculations include both the electrostatic and exchange-repulsion effects and he removes the dipole-induced-dipole contributions by appeal to a dielectric continuum model. He and Ishida have shown how to systematically build molecular polarization interaction potentials from *ab initio* calculations based on a variable charge scheme [20]. Recently an alternative, more readily applied method to obtain condensed phase polarizabilities from first-principles calculations has been proposed [21]. It can be applied to ions or molecules in arbitrary coordination environments and it was validated for a wide range of solid oxides.

In this paper we present an application of the latter method to several liquid phase systems. After a short description of the method in the framework of DFT calculations, we present, as a first example, calculations of the electronic polarizability of liquid water. We then studied two different ionic systems, namely a series of molten alkali fluorides (LiF, NaF, KF and CsF) and a series of four magmatic melts (silica, a rhyolite, the anorthite$_{0.36}$–diopside$_{0.64}$ eutectic mixture used as model basalt, and enstatite).

2. Numerical methods

2.1. Polarizabilities from DFT

DFT calculations on periodic systems are based on the Kohn–Sham (KS) method to determine the ground state electronic wavefunction at a given ionic configuration. One of its drawbacks is the delocalization of the electronic density throughout the whole simulation cell, which prevents any straightforward extraction of the individual electronic properties of a given atom or molecule.

The use of the maximally localized Wannier function (MLWF) formalism [22] is an efficient way to overcome this difficulty. The MLWFs provide a picture of the electron distribution around atoms which is easily interpretable from a chemical point of view. They are determined by unitary transformations of the KS eigenvectors

$$\phi_n^w(\mathbf{r}) = \sum_{m=1}^{J} U_{nm}|\phi_m\rangle, \tag{1}$$

where the sum runs over all the KS states $\{\phi_n\}_{n\in[1,J]}$, and the unitary matrix $\mathbf{U}$ is determined by iterative minimization of the Wannier function spread, which is defined by

$$\Omega = -\frac{1}{(2\pi)^2} w_\alpha \ln|z_\alpha|^2; \qquad z_\alpha = \langle\Psi|e^{i\frac{2\pi}{L}r_\alpha}|\Psi\rangle \tag{2}$$

when periodic boundary conditions are applied, where w_α are weights assigned to each axis x, y and z.

A complete theory of electric polarization in crystalline dielectrics has been developed in recent years [23–25], which validates the calculation of the dipole moments of single ions or molecules from the center of charge of the subset of MLWF which localize in the vicinity of them [26–28]. The MLWF centers are computed according to [26]

$$r_{n,\alpha}^w = \frac{L}{2\pi}\Im\left(\ln\langle\phi_n^w \mid e^{i\frac{2\pi}{L}r_\alpha}|\phi_n^w\rangle\right), \tag{3}$$

and the partial dipole moment for a given ionic or molecular species I is defined as

$$\boldsymbol{\mu}^I = \sum_{i\in I}\left(Z_i\mathbf{R}_i - 2\sum_{n\in i}\mathbf{r}_n^w\right). \tag{4}$$

When a small external electric field $\boldsymbol{\mathcal{E}}$ is applied to the media, the linear response may be characterized by an additional field-induced dipole moment $\boldsymbol{\delta\mu}^I$ on each individual species. It is convenient to think of the applied field as an optical field, in order to see how to distinguish its effect from that of the static fields which are caused by the permanent charge distributions of the molecules, and to think of $\boldsymbol{\delta\mu}^I$ as the net induced dipole which is oscillating at the optical frequency. For an electronically insulating material, the induced dipole

can be written in terms of the total (optical frequency) electric field which act on it,

$$\boldsymbol{\delta\mu}^I(\{\mathbf{R}^N\}) = \boldsymbol{\alpha}^I(\{\mathbf{R}^N\}) \cdot \left[\boldsymbol{\mathcal{E}} + \sum_{J \neq I} \hat{\mathbf{T}}^{IJ} \cdot \boldsymbol{\delta\mu}^J(\{\mathbf{R}^N\}) \right]. \quad (5)$$

In this equation, we have introduced the dipole polarizability tensor $\boldsymbol{\alpha}^I(\{\mathbf{R}^N\})$ of species I in the particular condensed phase configuration $\{\mathbf{R}^N\}$. It also contains the dipole–dipole interaction tensor, $\hat{\mathbf{T}}^{IJ}$, whose components are defined by $\hat{T}^{IJ}_{\alpha\beta} = \nabla_\alpha \nabla_\beta \frac{\hat{1}}{r^{IJ}}$; in practice, in a periodic system it will be computed with the Ewald summation technique [29]. The second-term on the right-hand side of the equation is the reradiated field from the dipoles induced in all the other molecules in the sample. In principle, higher order induced multipoles also contribute to this expansion but we will ignore them. In a uniform applied field the directly induced higher order multipoles on spherical atoms and ions vanish, and even for molecules their effect is expected to be much smaller than that of the dipoles.

In DFT calculations on periodic systems, the coupling between the external electric field and the electronic system is expressed through the macroscopic polarization of the periodically replicated cell [30, 31] and is defined using the Berry phase approach of Resta [32]. It is then possible to determine the new partial dipole moment for each species in the presence of a field, via another localization step. The dipoles induced by the field are calculated from the differences between the total molecular dipoles in the presence and absence of the field.

We can now invert equation (5) to determine the individual electronic polarizabilities for that particular condensed-phase configuration. Consider the application of fields $\boldsymbol{\mathcal{E}}^{(\alpha)}$, along each Cartesian direction $\alpha = x, y, z$ and denote by $\{\boldsymbol{\delta\mu}^{I,(\alpha)}\}_{I\in[1,N]}$, the corresponding calculated values of the induced dipole moments. We can then obtain values for the total field at each ion $\mathbf{f}^{I,(\alpha)}$, for each applied field direction from

$$\mathbf{f}^{I,(\alpha)} = \boldsymbol{\mathcal{E}}^{(\alpha)} + \sum_{J \neq I} \hat{\mathbf{T}}^{IJ} \cdot \boldsymbol{\delta\mu}^{J,(\alpha)}, \quad (6)$$

which is conveniently evaluated from the electric field given by a dipolar Ewald sum. We may then obtain the polarizability tensor of species I from

$$\boldsymbol{\alpha}^I(\{\mathbf{R}^N\}) = (\mathbf{F}^I)^{-1} \cdot \boldsymbol{\Pi}^I, \quad (7)$$

where $\mathbf{F}^I$ and $\boldsymbol{\Pi}^I$ are the 3×3 matrices,

$$F^I_{\alpha\beta} = f^{I,(\beta)}_\alpha \quad (8)$$

$$\Pi^I_{\alpha\beta} = \delta\mu^{I,(\beta)}_\alpha \quad (9)$$

and the subscripts refer to the Cartesian components of these vectors and tensors.

2.2. Computation details

Liquid water configurations were extracted from a density functional-based first-principle molecular dynamics simulation (FPMD) [33]. The simulated system was a periodically replicated box containing 32 water molecules at the experimental density. The gradient-corrected BLYP functional was used in conjunction with Troullier–Martins pseudo-potentials and a plane-wave basis-set with an energy cut-off of 70 Ryd. A small fictitious electron mass of 80 AU was used with a 2 AU time step. The system was first equilibrated at 350 K using a chain of three Nosé thermostats for 5 ps and then constant energy simulation was performed for 10 ps. We have chosen a temperature slightly higher than room temperature because it has been demonstrated that water described by FPMD has too high a melting temperature [34]. Unless specified, the computations were performed using the CPMD package [35].

Magmatic melts configurations were also extracted from FPMD simulations performed in similar conditions to the liquid water one. The compositions of the systems were the following:

- Silica: 32 Si and 64 O atoms, $V = 1451.89$ Å^3;
- Rhyolite: 26 Si, 5 Al, 3 Na, 2 K and 62 O atoms, $V = 1472.49$ Å^3;
- Enstatite: 20 Si, 20 Mg and 60 O atoms, $V = 1337.06$ Å^3;
- Anorthite$_{0.36}$–diopside$_{0.64}$: 18 Si, 6 Al, 6 Mg, 9 Ca and 60 O atoms, $V = 1344.91$ Å^3.

The temperature was set to 2500 K, and the densities were taken from literature data (see [36, 37] and references therein). 5 ps of constant energy simulation were generated after a 5 ps equilibration using a chain of Nosé thermostats. A minimum of 600 oxide ion individual polarizabilities were computed for each composition.

Finally, in the case of molten fluorides, configurations were extracted from a classical molecular dynamics simulation using a polarizable ion model potential [8, 38, 39], at several temperatures above the melting point, and corresponding experimental densities. Pure LiF, NaF, KF and CsF were studied, and a minimum of 300 individual polarizabilities were computed for each composition.

3. Results

3.1. Liquid water

Despite its key role in environmental sciences, biology and industrial technology, no universally satisfactory model potential has yet been built for liquid water. Most of the simulation work involves pairwise–additive, site–site potentials like TIP3P, TIP4P or SPC/E [40, 41], and these have been useful to describe water near ambient conditions (i.e. the conditions for which they have been calibrated) but often fail to reproduce quantities like the liquid–vapor coexistence curve [42]. The introduction of polarizable models does not improve very noticeably the simulated properties of bulk water under ambient conditions, but it has allowed important advances in the understanding of the solvation of ions or molecules [3, 43]. In the example already mentioned of molecular dynamics simulations of the liquid–vapor interface of salt-containing aqueous solutions, the

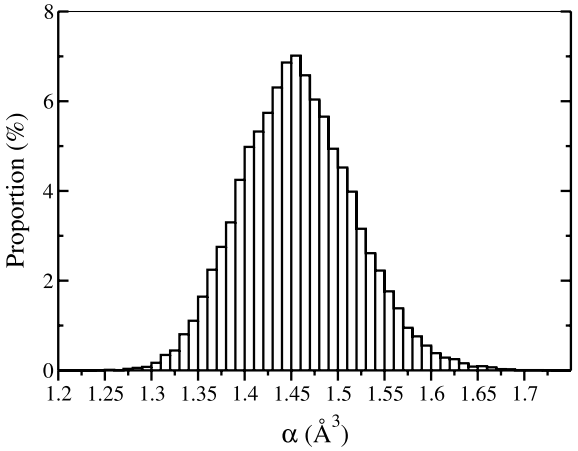

Figure 2. Distribution of the isotropic polarizabilities $\bar{\alpha}^I = \frac{1}{3}\mathrm{Tr}(\boldsymbol{\alpha}^I)$ of liquid water molecules.

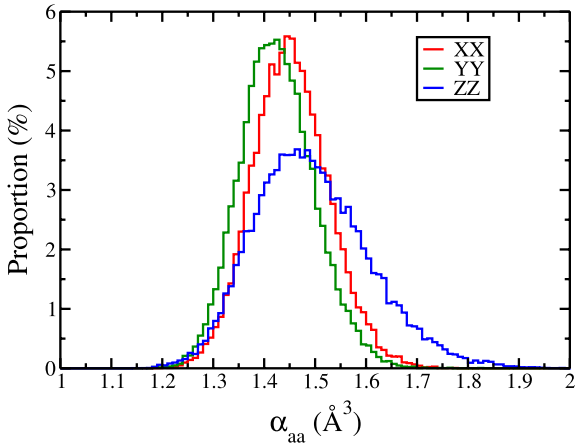

Figure 3. Distribution of the diagonal components α_{xx}, α_{yy} and α_{zz} of the polarizability tensor in liquid water (in the molecular framework, see the text for details).

inclusion of polarization effects was necessary to observe an affinity for the surface for the highly polarizable anions.

In recent years, many polarizable models have been reported, in which polarization effects are accounted for in different ways [44]. Because the polarizability of water is only known experimentally in the gas phase [45], this 'parameter' is set to a different value in each model. In the gas phase, in the molecular coordinate system (where the x axis is the H–O–H angle bisector, the y axis is the second axis in the molecular plane and the z axis therefore is perpendicular to the molecular plane), the polarizability tensor is nearly isotropic, and its diagonal components are $\alpha_{xx} = 1.47$ Å^3, $\alpha_{yy} = 1.53$ Å^3 and $\alpha_{zz} = 1.42$ Å^3. Many potentials therefore involve similar values (a selection of polarizable models with their corresponding parameters is given in reference [46]), but some important differences in the parameters can also be observed. For example, in several potentials the zz component of the polarizability is set to 0. Up to now, no systematic comparison has ever been made on the properties predicted by all these different models, but the liquid–air interface of salt-containing systems has been studied using two different models [1, 47], namely POL3 [48] and AMOEBA [49] (the latter also includes explicit higher order multipoles), and the results obtained for the ionic density profiles at the interface were in quantitative agreement one with each other. This indicates that, whilst it is important to include polarization effects, cancelation effects can occur between the various terms of the model potential, and it becomes difficult to trace back the influence of a parameter value on the physical chemistry of the system. By using a computed value for the polarizability, one source of arbitrariness could be removed in the potential building process.

In figure 2 we present the distribution obtained for the isotropic polarizabilities $\bar{\alpha}^I = \frac{1}{3}\mathrm{Tr}(\boldsymbol{\alpha}^I)$ of water molecules. The values of the polarizabilities of the individual molecules differ because of the differences in the configurations of their neighbors when we sample them from the liquid state simulations. The distribution is centered around a value of 1.46 Å^3, with respective minimum and maximum at 1.26 and 1.67 Å^3. No experimental value can be directly determined for this quantity in the liquid state, but it is possible to calculate the refractive index n from the Lorenz–Lorentz [50, 51] relationship:

$$\frac{n^2-1}{n^2+2} = \frac{4\pi}{3}\sum_I \rho^I \langle \bar{\alpha}^I \rangle. \tag{10}$$

where ρ^I is the number density of species I and $\langle \bar{\alpha}^I \rangle$ its average isotropic density (in the case of liquid water, only one species has to be considered). We then obtain a value of 1.33 for n, in perfect agreement with the experimental value [52]. The value obtained might be slightly overestimated since it has been shown that in the case of a gas phase water molecule that the use of BLYP functional leads to an overestimation of the polarizability [53]. The polarizability tensor was determined in the molecular framework, and the distribution of the diagonal components are given on figure 3. The average values are $\alpha_{xx} = 1.45$ Å^3 (1.47), $\alpha_{yy} = 1.42$ Å^3 (1.53) and $\alpha_{zz} = 1.48$ Å^3 (1.42), where the gas phase values are given in parentheses. As in the gas phase, the polarizability tensor is on average nearly isotropic. But the distributions obtained differ markedly, with a broader distribution for α_{zz}. To interpret this result, one can consider the shape of the electron cloud of a water molecule. The polarizability of a molecule or an ion is generally smaller in condensed phase than in the gas phase because of the presence of a confining potential due to the surrounding species. In the case of a water molecule, this confining potential will act more markedly in the plane of the molecule because of the presence of the three nuclei, and environmental effects therefore occur principally out of the plane, i.e. for the zz component of the polarizability tensor. Besides Silvestrelli and Parrinello have shown that in the liquid phase the distances between the oxygen atom and the Wannier centers along the OH covalent bond are slightly contracted with respect to the isolated molecule, while the lone pair orbitals (out-of-plane) are slightly pulled out [26].

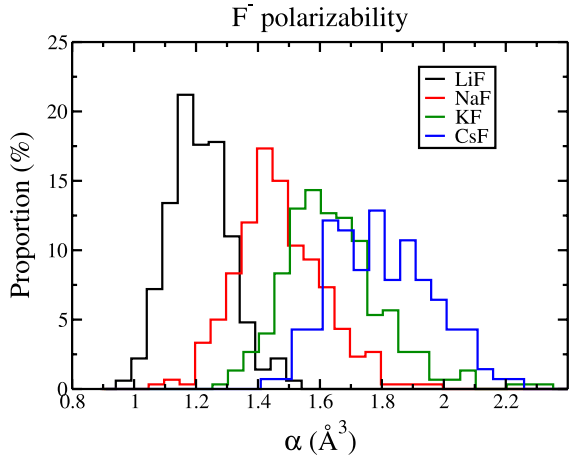

Figure 4. Distribution of the isotropic polarizabilities for F^- anion in various molten alkali fluorides.

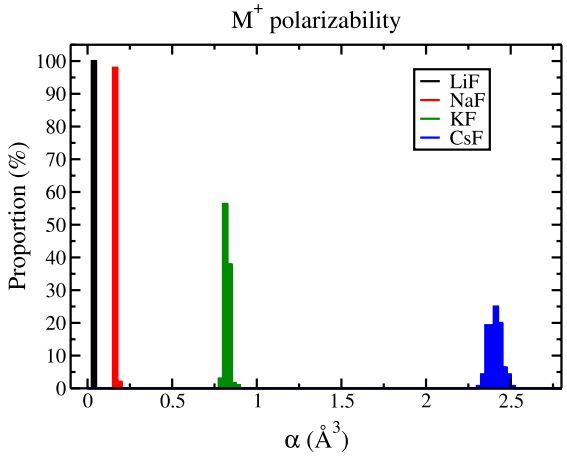

Figure 5. Distribution of the isotropic polarizabilities for cations in various molten alkali fluorides.

3.2. Molten fluorides

Fluoride-based molten salts are under intensive investigation because of their potential use in the nuclear industries of tomorrow. Despite their interesting neutronic and heat-transfer qualities, very few experimental studies have been undertaken to determine precisely their physico-chemical properties. This is due to their highly corrosive nature, which prevents easy measurement in the laboratory. Recently, we introduced polarizable interaction models for molecular dynamics simulations, which were shown to give a very accurate picture of the structure and dynamics of ions in those liquids where measurements are available for comparison. In these potentials, the polarizability (together with the other interaction potential parameters) were determined from first-principles via a dipole and force-matching procedure [38, 8]. In subsequent simulations, those potentials were able to reproduce transport properties like the electrical conductivity or the viscosity [9, 13, 54] as well as thermodynamic properties like the surface tension [55].

In this work we focused on the series of alkali fluorides in order to evaluate the influence of the nature of the cation on the anion polarizability. It is well established that environmental effects are very important in ionic systems [56, 57, 21]. Most of the work which has been undertaken used cluster models of the crystalline environment and it has been shown that the anion polarizability varies from one crystal to another. For a given crystal important variations could also be observed when changing the pressure, and thus the lattice parameter of the crystal.

In each of the four systems we have studied, namely LiF, NaF, KF and CsF, the polarizability tensors are almost isotropic and we obtain a centered distribution for the isotropic polarizabilities of the anions (figure 4). The center of the distribution shifts a lot from one alkali cation to another, passing from 1.15 $Å^3$ in LiF (which is very close to the fitted value used in our previous work on mixtures of LiF with BeF_2) to 1.75 $Å^3$ in CsF. The confining potential, which affects the electron density around a given anion, originates from both Coulombic interactions and the exclusion of electrons from the region occupied by the electron density of the first-neighbor shell of cations [58]. When passing from one cation to another (for example in the series $Li^+ \rightarrow Na^+ \rightarrow K^+ \rightarrow Cs^+$), two effects are then competing: on the one hand, the anion–cation distance increases, which results in a diminution of the confining potential, but on the other hand, the volume occupied by the cation electron density also increases, with an opposite effect on the confining potential. Here, the observed increase of polarizability with the size of the cation tends to show that the first effect is the most important. Indeed, the value obtained for CsF is approaching the free F^- anion polarizability, which is 2.37 $Å^3$.

We also determined polarizabilities for all the cations; these are displayed on figure 5. All the distributions are much narrower than the corresponding F^- ones, and the average values for the polarizabilities are 0.04 $Å^3$ for Li^+, 0.16 $Å^3$ for Na^+, 0.82 $Å^3$ for K^+ and 2.41 $Å^3$ for Cs^+ ions, and there is a progressive increase of this quantity with the alkali cation size. Note that in the literature there is a long-standing effort to determine ionic polarizabilities in various ionic systems (mostly crystalline) through the knowledge of refractive indices. A recent model calculation [59] proposes a list of empirical electronic polarizabilities in 650 ionic systems including 51 fluorides. the recommended values are 1.295 $Å^3$ for F^- anion and 0.19, 0.309, 0.988 $Å^3$ for Li^+, Na^+ and K^+ cations. It is clear that this approach has some limitation since the electronic polarizability of ions in condensed phase is very sensitive to the composition and pressure of the system. Some high level all-electron quantum calculations on embedded clusters [60] gave values of 0.0266, 0.143 and 0.791 $Å^3$ for Li^+, Na^+ and K^+ cations, which are in good agreement with our values and substantially smaller than the empirical ones.

3.3. Magmatic melts

Magmatic melts are natural silicate systems which are composed of a number of major oxides (up to nine), silica being the most important one. They are considered as ionic liquids, in which the anion is the oxide ion, O^{2-}.

From the Earth's crust to its lower mantle, the variation of composition is large. For this reason it would be very difficult to perform experiments on each different system with varying temperature and pressure, and which gives a strong motivation for the development of simulations of these systems. In the most recent work, two different approaches to constructing potentials are apparent. First, a very simple interionic potential was developed to describe the nine component system K_2O–Na_2O–CaO–MgO–FeO–Fe_2O_3–Al_2O_3–TiO_2–SiO_2 [36, 37]. This potential reproduced satisfactorily a number of thermodynamics, structural and transport properties of a representative set of natural silicate melts. Good transferability was obtained, although accuracy was limited for silica-rich and iron-rich melts. The second approach is similar to the one already mentioned for molten fluoride systems; it involves a fully flexible ionic interaction model (Aspherical Ion Model, AIM, in which dipole and quadrupole polarization effects are also included) and it was applied to various relevant minerals and melts of the CaO–MgO–Al_2O_3–SiO_2 (CMAS) system [61]. Its transferability range was tested over a wide range of temperature and pressure conditions. The drawback of this method is that the accessible simulation system sizes and durations are smaller than with the simple pair potential. Its advantage is that it can reproduce thermodynamic and structural properties in very good agreement with experiments in almost all the studied compositions. An example of comparison of the total static and dynamic structure factors for liquid alumina with the AIM model are given in [10].

Oxide ion polarizabilities have already been determined for crystalline systems [21], using the same method as applied here. It was shown that the anion polarizability was varying substantially when passing from SiO_2 or Al_2O_3 to BaO. In the case of magmatic melts, which mainly contain SiO_2, the variation should be less important. The distribution obtained for the polarizabilities in anorthite–diopside mixture, enstatite, rhyolite and pure silica are given in figure 6. As in the case of molten fluorides, we observe important environmental effects. In this case, the shift in the center of the distribution center is smaller, but the widths of the distributions change a lot from one system to another. In pure silica and in rhyolite, which is the mixture richest in silica, isotropic polarizabilities are well distributed around their respective average values of 1.48 and 1.54 $Å^3$. In the case of enstatite and even more markedly of the model basalt (anorthite–diopside mixture), the distributions become very broad (we can extract average values of 1.84 $Å^3$ and $\approx$2.0 $Å^3$ respectively). In the case of these complex mixtures which involve several cationic species, the oxide anions sample many different environments. For example, some of them are bridging oxygens (BO) linking two Si atoms (or Al in alumino silicates) as they would in pure silica (see figure 1), while some others are non-bridging oxygens (NBO) as they connect only one network former cation (Si or Al) to one or several network modifier cations (alkali or alkaline earth cations). When they are BOs, the two Wannier orbitals involved into the strong Si–O bonds are weakly polarizable whereas the lone pair orbitals are free to localize. The overall result is a rather low average polarizability. On the contrary

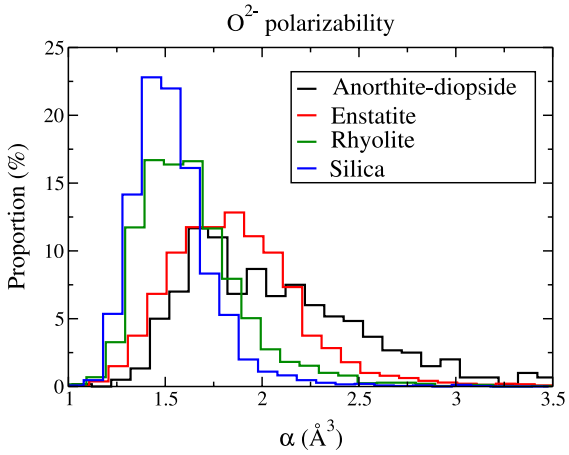

Figure 6. Distribution of the isotropic polarizabilities for O^{2-} anion in various magmatic melts.

for a NBO only one Wannier orbital is connected to a Si (or Al) atom while the three other orbitals are more loosely linked to low field cations located in the neighborhood. The result is on average a greater polarizability of the oxygen. Knowing that the number of NBO increases drastically with the content in network modifier cations (for a discussion see [62]) the value of the polarizability increases with the degree of depolymerization of the melt, i.e. in the following series: silica, rhyolite, anorthite–diopside and finally enstatite.

4. Conclusion

The calculation of the response of the electron density of a condensed phase to an applied external field in the framework of density functional theory has allowed a systematic determination of the polarizabilities of individual molecules and ions in several liquids. The method rests on the use of the transformation of the electric field perturbed Kohn–Sham orbitals to localized Wannier functions which are then used to extract the induced dipole on each molecule. It had already been successfully tested on another type of condensed phase material, namely a series of oxide crystals [21]. The method will allow, *inter alia*, values for the polarizability for use in polarizable simulation potentials to be determined independently of considerations of forces, energies etc.

For liquid water, a distribution centered around a value of 1.46 $Å^3$ was obtained, and the polarization tensor was found to be nearly isotropic in the molecular frame. In the case of the fluoride and oxide anions in ionic liquids, several environment types were studied by varying the corresponding counterions in the liquids. The mean anion polarizabilities increased with the decreasing strength of the confining potential exerted by neighboring cations. For example, the polarizability of the F^- ion varied from 1.15 $Å^3$ in molten LiF to 1.75 $Å^3$ in molten CsF. As exemplified by the fluorides, the liquid phase anion polarizabilities were larger than the values obtained for the corresponding crystal (0.98 $Å^3$ for crystalline LiF [63]). In the molten silicates, substantial variations in the mean polarizability of the oxide ion were

found between different melt compositions. These results suggest that the properties predicted with polarizable potentials could be improved by allowing for these variations between phases and compositions, making use of the results from the present polarizability calculation method. Furthermore, the values of the polarizability for different ions in the same liquid showed very substantial variations, especially in the oxides; these fluctuations are due to differences in the instantaneous environmental potential. This suggests that a fully transferable interaction potential, giving an accurate account of the polarization effects, should account for these fluctuations in the polarizabilities of the individual ions. A first attempt of building such potentials was already reported for crystalline MgO [64, 65]. In water, the amplitude of the polarizability fluctuations was considerably smaller than in the ionic liquids, showing that the representation of the polarization effects through a mean polarizability should work well in molecular liquids. We note, in passing, that these polarizability fluctuations are directly observable in the light-scattering spectrum of a liquid, so that calculations like those described here can be used as first-principles input to a calculation of the light-scattering spectrum [66].

In future work we will study some more complex liquid systems, for which very little is known concerning individual polarizabilities. For example, in the room temperature ionic liquids, the overwhelming majority of the simulation work employs non-polarizable force fields [67], and it is believed that the inclusion of polarization effects would enhance significantly the quality of the predicted physico-chemical properties [68, 69]. We will also focus on the study of solutes in molecular or ionic liquids. Indeed, an interesting feature of our method is its applicability to any molecule in a solvent, with the usual drawback of the need to perform more calculations to reach acceptable statistical accuracy. In the case of aqueous solutions, it would be valuable to determine the polarizabilities of several series of ions, to address the problems described in the introduction. In the case of magmatic melts, the nature of the interesting solutes is somewhat different. The solubility of noble gases in magmas is important to understand the outgassing of the Earth's mantle [70]. The knowledge of their polarizability in such an environment would not only allow one to build a polarizable potential for those systems (noble gas + silicate melt), but it would also help to refine the simple pair potentials that have already been used. Here the dispersion terms, which play an important role for the species solubility, can be determined from the polarizability through the use of Slater–Kirkwood or similar relationship [71].

References

[1] Jungwirth P and Tobias D J 2002 Ions at the air/water interface *J. Phys. Chem.* B **106** 6361–73

[2] Dang L X and Chang T-M 2002 Molecular mechanism of ion binding to the liquid/vapor interface of water *J. Phys. Chem.* B **106** 235–8

[3] Jungwirth P and Tobias D J 2006 Specific ion effects at the air/water interface *Chem. Rev.* **106** 1259–81

[4] Padmanabhan V, Daillant J, Belloni L, Mora S, Alba M and Konovalov O 2007 Specific ion adsorption and short-range interactions at the air aqueous solution interface *Phys. Rev. Lett.* **99** 086105

[5] Kunz W, Lo Nostro P and Ninham B W 2004 The present state of affairs with Hofmeister effects *Curr. Opin. Colloid Interface Sci.* **9** 1–18

[6] Hutchinson F, Rowley A J, Walters M K, Wilson M, Madden P A, Wasse J C and Salmon P S 1999 Structure of molten MCl_3 systems from a polarizable ion simulation model *J. Chem. Phys.* **111** 2028–37

[7] Salanne M, Simon C, Turq P and Madden P A 2008 Calculation of activities of ions in molten salts with potential application to the pyroprocessing of nuclear waste *J. Phys. Chem.* B **112** 1177–83

[8] Heaton R J, Brookes R, Madden P A, Salanne M, Simon C and Turq P 2006 A first-principles description of liquid BeF_2 and its mixtures with LiF:1. potential development and pure BeF_2 *J. Phys. Chem.* B **110** 11454–60

[9] Salanne M, Simon C, Turq P, Heaton R J and Madden P A 2006 A first-principles description of liquid BeF_2 and its mixtures with LiF: 2. Network formation in LiF–BeF_2 *J. Phys. Chem.* B **110** 11461–7

[10] Jahn S and Madden P A 2007 Structure and dynamics in liquid alumina: simulations with an *ab initio* interaction potential *J. Non-Cryst. Solids* **353** 3500–4

[11] Wilson M, Madden P A, Hemmati M and Angell C A 1996 Polarization effects, network dynamics, and the infrared spectrum of amorphous SiO_2 *Phys. Rev. Lett.* **77** 4023–6

[12] Brookes R, Davies A, Ketwaroo G and Madden P A 2005 Diffusion coefficients in ionic liquids: relationship to the viscosity *J. Phys. Chem.* B **109** 6485–90

[13] Salanne M, Simon C, Turq P and Madden P A 2007 Conductivity–viscosity-structure: unpicking the relationship in an ionic liquid *J. Phys. Chem.* B **111** 4678–84

[14] Remler D K and Madden P A 1990 Molecular dynamics without effective potentials via the car-parrinello approach *Mol. Phys.* **70** 921–66

[15] Vuilleumier R 2006 Density functional theory based *ab initio* molecular dynamics using the car-parrinello approach *Lect. Notes Phys.* **703** 223–85

[16] Jungwirth P and Tobias D J 2002 Chloride anion on aqueous clusters, at the air–water interface, and in liquid water: solvent effects on Cl^- polarizability *J. Phys. Chem.* A **106** 379–83

[17] Jungwirth P, Curtis J E and Tobias D J 2003 Polarizability and aqueous solvation of the sulfate dianion *Chem. Phys. Lett.* **367** 704–10

[18] Salvador P, Curtis J E, Tobias D J and Jungwirth P 2003 Polarizability of the nitrate anion and its solvation at tha air/water interface *Phys. Chem. Chem. Phys.* **5** 3752–7

[19] Morita A 2002 Water polarizability in condensed phase: *ab initio* evaluation by cluster approach *J. Comput. Chem.* **23** 1466–71

[20] Ishida T and Morita A 2006 Extended treatment of charge response kernel comprising the density functional theory and charge regulation procedures *J. Chem. Phys.* **125** 074112

[21] Heaton R J, Madden P A, Clark S J and Jahn S 2006 Condensed phase ionic polarizabilities from plane wave density functional theory calculations *J. Chem. Phys.* **125** 144104

[22] Marzari N and Vanderbilt D 1997 Maximally localized generalized wannier functions for composite energy bands *Phys. Rev.* B **56** 12847–65

[23] King-Smith R D and Vanderbilt D 1993 Theory of polarization of crystalline solids *Phys. Rev.* B **47** 1651–4

[24] Vanderbilt D and King-Smith R D 1993 Electric polarization as a bulk quantity and its relation to surface charge *Phys. Rev.* B **48** 4442–55

[25] Souza I, Wilkens T and Martin R M 2000 Polarization and localization in insulators: generating function approach *Phys. Rev.* B **62** 1666–83

[26] Silvestrelli P L and Parrinello M 1999 Water molecule dipole in the gas and in the liquid phase *Phys. Rev. Lett.* **82** 3308–11

[27] Bernasconi L, Wilson M and Madden P A 2001 Cation polarizability from first-principles: Sn^{2+} *Comput. Mater. Sci.* **22** 94–8

[28] Bernasconi L, Madden P A and Wilson M 2002 Ionic to molecular transition in $AlCl_3$: an examination of the electronic structure *PhysChemComm* **5** 1–11

[29] Aguado A and Madden P A 2003 Ewald summation of electrostatic multipole interactions up to the quadrupolar level *J. Chem. Phys.* **119** 7471–83

[30] Umari P and Pasquarello A 2002 *Ab initio* molecular dynamics in a finite homogeneous electric field *Phys. Rev. Lett.* **89** 157602

[31] Umari P and Pasquarello A 2005 Density functional theory with finite electric field *Int. J. Quantum. Chem.* **101** 666–70

[32] Resta R 1998 Quantum-mechanical position operator in extended systems *Phys. Rev. Lett.* **80** 1800–3

[33] Car R and Parrinello M 1985 Unified approach for molecular dynamics and density-functional theory *Phys. Rev. Lett.* **55** 2471–4

[34] Sit P H-L and Marzari N 2005 Static and dynamic properties of heavy water at ambient conditions from first-principles molecular dynamics *J. Chem. Phys.* **122** 204510

[35] CPMD http://www.cpmd.org/ Copyright IBM Corp 1990–2008, Copyright MPI Für Festkörperforschung Stuttgart 1997–2001

[36] Guillot B and Sator N 2007 A computer simulation study of natural silicate melts. Part I: low pressure properties *Geochim. Cosmochim. Acta* **71** 1249–65

[37] Guillot B and Sator N 2007 A computer simulation study of natural silicate melts. Part II: high pressure properties *Geochim. Cosmochim. Acta* **71** 4538–56

[38] Madden P A, Heaton R, Aguado A and Jahn S 2006 From first-principles to material properties *J. Mol. Struct.: THEOCHEM* **771** 9–18

[39] Salanne M, Simon C, Turq P and Madden P A 2008 Heat-transport properties of molten fluorides: determination from first-principles *J. Fluorine Chem.* doi:10.1016/j.jfluchem.2008.07.013

[40] Jorgensen W L, Chandrasekhar J, Madura J D, Impey R W and Klein M L 1983 Comparison of simple potential functions for simulating liquid water *J. Chem. Phys.* **79** 926–35

[41] Berendsen H J C, Grigera J R and Straatsma T P 1987 The missing term in effective pair potentials *J. Chem. Phys.* **91** 6269–71

[42] Guillot B and Guissani Y 2001 How to build a better pair potential for water *J. Chem. Phys.* **114** 6720–33

[43] Houriez C, Ferre N, Masella M and Siri D 2008 Prediction of nitroxide hyperfine coupling constants in solution from combined nanosecond scale simulations and quantum computations *J. Chem. Phys.* **128** 244504

[44] Yu H and van Gunsteren W F 2005 Accounting for polarization in molecular simulation *Comput. Phys. Commun.* **172** 69–85

[45] Murphy W F 1977 The Rayleigh depolarization ratio and rotational Raman spectrum of water vapor and the polarizability components for the water molecule *J. Chem. Phys.* **67** 5877–82

[46] Schropp B and Tavan P 2008 The polarizability of point-polarizable water models: density functional theory/molecular mechanics results *J. Phys. Chem.* B **112** 6233–40

[47] Tuma L, Jenicek D and Jungwirth P 2005 Propensity of heavier halides for the water/vapor interface revisited using the Amoeba force field *Chem. Phys. Lett.* **411** 70–4

[48] Caldwell J W and Kollman P A 1995 Structure and properties of neat liquids using nonadditive molecular dynamics: water, methanol, and *N*-methylacetamide *J. Phys. Chem.* **99** 6208–19

[49] Ren P and Ponder J W 2003 Polarizable atomic multipole water model for molecular mechanics simulation *J. Phys. Chem.* B **107** 5933–47

[50] Lorenz L 1880 Ueber die refractionsconstante *Ann. Phys., Lpz.* **247** 70–103

[51] Lorentz H A 1880 Ueber die beziehung zwischen der fortpflanzungsgeschwindigkeit des lichtes und der körperdichte *Ann. Phys., Lpz.* **245** 641–65

[52] Harvey A H, Gallagher J S and Levelt Sengers J M H 1998 Revised formulation for the refractive index of water and steam as a function of wavelength, temperature and density *J. Phys. Chem. Ref. Data* **27** 761–73

[53] Umari P and Pasquarello A 2003 Polarizabilty and dielectric constant in density-functional supercell calculations with discrete *k*-point samplings *Phys. Rev.* B **68** 085114

[54] Salanne M, Simon C, Groult H, Lantelme F, Goto T and Barhoun A 2008 Transport in molten lif-naf-zrf4 mixtures: a combined computational and experimental approach *J. Fluorine Chem.* doi:10.1016/j.jfluchem.2008.07.005

[55] Salanne M, Simon C, Turq P and Madden P A 2007 Simulation of the liquid–vapor interface of molten $LiBeF_3$ *C.R. Chim.* **10** 1131–6

[56] Wilson J N and Curtis R M 1970 Dipole polarizabilities of ions in alkali halide crystals *J. Phys. Chem.* **74** 187–96

[57] Wilson M, Madden P A, Jemmer P, Fowler P W, Batana A, Bruno J, Munn R W and Monard M C 1999 Models of environmental effects on anion polarizability *Mol. Phys.* **96** 1457–67

[58] Jemmer P, Fowler P W, Wilson M and Madden P A 1998 Environmental effects on anion polarizability: variation with lattice parameter and coordination number *J. Phys. Chem.* A **102** 8377–85

[59] Shannon R D and Fischer R X 2006 Empirical electronic polarizabilities in oxides, hydroxides, oxyfluorides, and oxychlorides *Phys. Rev.* B **73** 235111

[60] Domene C, Fowler P W, Madden P A, Xu J, Wheatley R J and Wilson M 2001 Short-range contributions to the polarization of cations *J. Phys. Chem.* A **105** 4136–42

[61] Jahn S and Madden P A 2007 Modeling Earth materials from crustal to lower mantle conditions: a transferable set of interaction potentials for the CMAS system *Phys. Earth Planet. Inter.* **162** 129–39

[62] Vuilleumier R, Sator N and Guillot B 2008 Computational modeling of natural silicate melts: what can we learn from *ab initio* simulations at press

[63] Heaton R J 2007 From first-principles to material properties *PhD Thesis* University of Oxford

[64] Aguado A and Madden P A 2004 Fully transferable interatomic potentials for large-scale computer simulations of simple metal oxides: application to MgO *Phys. Rev.* B **70** 245103

[65] Aguado A and Madden P A 2005 New insights into the melting behavior of MgO from molecular dynamics simulations: the importance of premelting effects *Phys. Rev. Lett.* **94** 068501

[66] Heaton R J and Madden P A 2008 Fluctuating ionic polarizabilities in the condensed phase: first-principles calculations of the Raman spectra of ionic melts *Mol. Phys.* **106** 1703–19

[67] Schroder C and Steinhauser O 2008 The influence of electrostatic forces on the structure and dynamics of molecular ionic liquids *J. Chem. Phys.* **128** 224503

[68] Resente Prado C E, Del Popolo M G, Youngs T G A, Kohanoff J and Lynden-Bell R M 2006 Molecular electrostatic properties of ions in an ionic liquid *Mol. Phys.* **104** 2477–83

[69] Yan T, Li S, Jiang W, Gao X, Xiang B and Voth G A 2006 Structure of the liquid–vacuum interface of room-temperature ionic liquids: a molecular dynamics study *J. Phys. Chem.* B **110** 1800–6

[70] Guillot B and Sarda P 2006 The effect of compression on noble gas solubility in silicate melts and consequences for degassing at mid-ocean ridges *Geochim. Cosmochim. Acta* **70** 1215–30

[71] Becke A D and Johnson E R 2007 Exchange-hole dipole moment and the dispersion interaction revisited *J. Chem. Phys.* **127** 154108